AIAA JOURNAL
Vol. 39, No. 2, February 2001

Dynamic Flexibility Method for Extracting Constrained Structural Modes from Free Test Data

Fuqiang Liu*
Nanjing University of Aeronautics and Astronautics, 210016 Nanjing, People's Republic of China
De-Wen Zhang†
Beijing Institute of Structure and Environment, 100076 Beijing, People's Republic of China
and
Lingmi Zhang‡
Nanjing University of Aeronautics and Astronautics, 210016 Nanjing, People's Republic of China

A method for extracting constrained modes from free-boundary modal test data is developed as an alternate approach when the constrained modal survey proves difficult. The transformation relationship between the modes of a free–free structure and those of a corresponding constrained structure is described, and a nonlinear characteristic equation is derived. Then an eigenvalue shifting technique, which can also improve computational efficiency, is employed to avoid the singularity of the stiffness matrix of free structures. The method utilizes a subset of measurable lower-order free modes plus the effects of neglected higher-order modes on the dynamic flexibility matrix. However, the analytical or measured higher-order modes of a free structure are unknown or difficult to obtain, and so the contribution of the higher-order modes to the dynamic flexibility matrix is expanded as a power series. The constrained modes are obtained by solving the nonlinear characteristic equation. It will be seen that this method is a typical substitute for the procedures based on experimental and theoretical modeling. Numerical simulation demonstrates that the method can converge quickly and has satisfactory precision.

Nomenclature

$A_0, \bar{A}_0, A_1, \bar{A}_1, \ldots$	=	(n, n) matrices to be determined
F	=	(n, n) dynamic flexibility matrix
F_h	=	(n, n) dynamic flexibility matrix of higher-order modes
K	=	(n, n) symmetric semidefinite positive stiffness matrix
K^*	=	(n, n) shifted stiffness matrix
$\bar{K}$	=	(k, k) transformed stiffness matrix
M	=	(n, n) symmetric positive difnite mass matrix
$\bar{M}$	=	(k, k) transformed mass matrix
$\Delta\lambda$	=	eigenvalue shifting value
Λ_h	=	(h, h) higher-order free–free frequencies
Λ_h^*	=	(h, h) shifted higher-order free–free frequencies
Λ_k	=	(k, k) lower-order free–free frequencies
Λ_k^*	=	(k, k) shifted lower-order free–free frequencies
λ_{hs}	=	sth higher-order free–free frequencies
λ_{hs}^*	=	sth higher-order free–free frequencies after shifted
λ_{ks}	=	sth lower-order free–free frequencies
ϕ_h	=	(n, h) higher-order free–free modes
ϕ_k	=	(n, k) lower-order free–free modes
ψ	=	(n, k) transformation matrix
$\|\cdot\|$	=	2-norm
$\|\cdot\|$	=	absolute

Subscripts and Superscripts

b	=	number of boundary degrees of freedom
c	=	number of constrained modes and frequencies
h	=	number of higher-order free–free modes
i	=	number of internal degrees of freedom
k	=	number of lower-order free–free modes
n	=	number of degrees of freedom for a free system
r	=	number of rigid-body modes
$*$	=	shifted quantities

Received 21 May 1999; revision received 21 September 1999; accepted for publication 2 August 2000.

*Research Assistant, Institute of Vibration Engineering, P.O. Box 333.
†Professor and Senior Research Engineer, First Research Division, P.O. Box 9210. Member AIAA.
‡Professor, Institute of Vibration Engineering, P.O. Box 333.

I. Introduction

APPROACHES for extracting free–free (free-boundary) modes from constrained test data have been studied in Refs. 1–4. However, some difficulties have been experienced in the constrained modal test. As stated in Refs. 5 and 6, it is difficult to have a truly fixed-base test because of the coupling between the test article and the fixture. Furthermore, designing and manufacturing a fixture is laborsome, even prohibitive for some structures. The alternative method, free-boundary modal test techniques that extract constrained modes from free test data, will be convenient for engineering applications.

Some papers have reported investigations of the free-boundary modal test method. Blair and Vadlamudi[5] presented a useful method where the minima of the interface response functions were used to obtain a shuttle-constrained space telescope model for loads analysis. The method is simple to use, but the constrained mode shapes cannot be derived directly. Admire et al.[6] developed a mass-additive modal test method, which uses free-boundary mass-added modes along with analytical mass and stiffness matrices. Although the mass-loaded method converges much more quickly, it requires a lot of mass-additive test modes for some structures. This imposes some difficulties in a modal test. A residual flexibility test method was also proposed.[7] In this approach, the residual effects of neglected higher-order modes are considered; thus, the number of free test modes can be greatly reduced. Nevertheless, it is difficult to obtain the residual flexibility matrix by a modal test. In addition, it is also troublesome to compute the residual flexibility matrix because of the singularity of the stiffness matrix of a free structure.

A new method for extracting constrained modes from free test data based on dynamic flexibility is developed in this paper. Two methods for computing the effects of neglected higher-order modes on the dynamic flexibility are discussed: one is a power series expansion method,[8] and the other is a residual dynamic flexibility method.[9] They both use free test modes plus the effects of neglected higher-order modes on dynamic flexibility. Only the former is

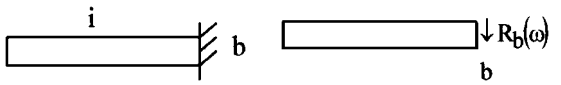

a) Constrained structure **b) Free structure**

Fig. 1 Structural system.

discussed in detail and is applied to a truss structure with closely spaced frequencies. Numerical example demonstrates that the method for extracting constrained modes from free test data is applicable. The effectiveness of the model will be determined after the method is verified under the condition that the error of mode expansion and measurement is introduced or even verified by the real modal test data. These issues will be addressed in the future.

II. Problem Formulation

In Fig. 1a, if the constrained structure harmonically vibrates at the frequency ω, it can be viewed as a harmonic force $R_b(\omega)$ that exists at the boundary. When its boundary is emancipated, the constrained structure will be equivalent to a free one that is excited by the boundary force $R_b(\omega)$ (Fig. 1b). Then the equation of motion for the free structure is

$$\begin{bmatrix} M_{ii} & M_{ib} \\ M_{bi} & M_{bb} \end{bmatrix} \begin{Bmatrix} \ddot{X}_i \\ \ddot{X}_b \end{Bmatrix} + \begin{bmatrix} K_{ii} & K_{ib} \\ K_{bi} & K_{bb} \end{bmatrix} \begin{Bmatrix} X_i \\ X_b \end{Bmatrix} = \begin{Bmatrix} 0 \\ R_b(\omega) \end{Bmatrix} \tag{1}$$

where $R_b(\omega) = R_b e^{j\omega t}$, $X = x e^{j\omega t}$, and t is time. Equation (1) can be written as

$$\begin{bmatrix} K_{ii} & K_{ib} \\ K_{bi} & K_{bb} \end{bmatrix} \begin{Bmatrix} x_i \\ x_b \end{Bmatrix} - \bar{\omega} \begin{bmatrix} M_{ii} & M_{ib} \\ M_{bi} & M_{bb} \end{bmatrix} \begin{Bmatrix} x_i \\ x_b \end{Bmatrix} = \begin{Bmatrix} 0 \\ R_b \end{Bmatrix} \tag{2}$$

in which $\bar{\omega} = \omega^2$. Equation (2) can be reduced to

$$(K - \bar{\omega} M)x = R \tag{3}$$

Whereas the characteristic equation for the free structure as shown in Fig. 1b is

$$(K - \lambda M)\varphi = 0 \tag{4}$$

and the characteristicequation for the constrainedstructure in Fig. 1a is given by

$$(K_{ii} - \bar{\omega} M_{ii})x_i = 0 \tag{5}$$

When it is assumed that the free test eigenpairs are Λ_k and ϕ_k and that the higher-order analytical eigenpairs from Eq. (4) are Λ_h and ϕ_h the displacement response x in Eq. (3) can be represented as a linear combination of lower-order test modes ϕ_k and higher-order analytical modes of the free structure,

$$x = \phi_k q_k + \phi_h q_h = \phi q \tag{6}$$

in which

$$\phi = [\phi_k, \phi_h], \qquad q = \begin{Bmatrix} q_k \\ q_h \end{Bmatrix} \tag{7}$$

Substituting Eq. (6) into Eq. (3) yields

$$\begin{bmatrix} \Lambda_k & 0 \\ 0 & \Lambda_h \end{bmatrix} \begin{Bmatrix} q_k \\ q_h \end{Bmatrix} - \bar{\omega} \begin{bmatrix} I_k & 0 \\ 0 & I_h \end{bmatrix} \begin{Bmatrix} q_k \\ q_h \end{Bmatrix} = \begin{Bmatrix} \phi_k^T R \\ \phi_h^T R \end{Bmatrix} \tag{8}$$

where $\Lambda_k = \phi_k^T K \phi_k$, $I_k = \phi_k^T M \phi_k$, $\Lambda_h = \phi_h^T K \phi_h$, and $I_h = \phi_h^T M \phi_h$. From the second row of Eq. (8),we have

$$\Lambda_h q_h - \bar{\omega} I_h q_h = \phi_h^T R \tag{9}$$

Hence,

$$q_h = (\Lambda_h - \bar{\omega} I_h)^{-1} \phi_h^T R \tag{10}$$

Embedding Eq. (10) into Eq. (6) gives

$$x = \phi_k q_k + F_h(\bar{\omega}) R \tag{11}$$

where

$$F_h(\bar{\omega}) = \phi_h (\Lambda_h - \bar{\omega} I_h)^{-1} \phi_h^T \tag{12}$$

is known as residual dynamic flexibility. Equation (11) can be partitioned as

$$\begin{Bmatrix} x_i \\ x_b \end{Bmatrix} = \begin{bmatrix} \phi_{ki} \\ \phi_{kb} \end{bmatrix} q_k + \begin{bmatrix} F_{h,ii} & F_{h,ib} \\ F_{h,bi} & F_{h,bb} \end{bmatrix} \begin{bmatrix} 0 \\ R_b \end{bmatrix} \tag{13}$$

that is,

$$x_i = \phi_{ki} q_k + F_{h,ib} R_b \tag{14a}$$

$$x_b = \phi_{kb} q_k + F_{h,bb} R_b \tag{14b}$$

For the constrained structure in Fig. 1a, we have the following equation:

$$x_b = 0 \tag{15}$$

Inserting Eq. (14b) into Eq. (15) yields

$$R_b = -F_{h,bb}^{-1} \phi_{kb} q_k \tag{16}$$

Equation (11) can be rewritten as

$$x = \phi_k q_k + [F_{h,i} \quad F_{h,b}] \begin{Bmatrix} 0 \\ R_b \end{Bmatrix} \tag{17}$$

in which

$$F_{h,i} = \begin{bmatrix} F_{h,ii} \\ F_{h,bi} \end{bmatrix}, \qquad F_{h,b} = \begin{bmatrix} F_{h,ib} \\ F_{h,bb} \end{bmatrix} \tag{18}$$

Substituting Eq. (16) into Eq. (17), we have

$$\begin{aligned} x &= \phi_k q_k + F_{h,b} R_b \\ &= \phi_k q_k - F_{h,b} F_{h,bb}^{-1} \phi_{kb} q_k \\ &= \psi q_k \end{aligned} \tag{19}$$

where

$$\psi = \phi_k - F_{h,b} F_{h,bb}^{-1} \phi_{kb} \tag{20}$$

Combining Eq. (19) and Eq. (3) yields

$$[\bar{K}(\bar{\omega}) - \bar{\omega} \bar{M}(\bar{\omega})] q_k = \psi^T R = 0 \tag{21}$$

where

$$\bar{K}(\bar{\omega}) = \psi^T K \psi, \qquad \bar{M}(\bar{\omega}) = \psi^T M \psi \tag{22}$$

It is easy to verify that $\psi^T R = 0$ in Eq. (21).

Equation (21) is a nonlinear characteristic equation because $F_h(\bar{\omega})$ is a nonlinear function of $\bar{\omega}$. After solving Eq. (21), the constrained frequencies ω_c, that is, frequency ω, and the partition factor q_k can be obtained. Then the force $R_b(\omega)$ can be computed from Eq. (16). Finally, the constrained modes can be obtained from Eq. (14a) as

$$x_c = \left(\phi_{ki} - F_{h,ib} F_{h,bb}^{-1} \phi_{kb}\right) q_k \tag{23}$$

III. Computation of Dynamic Flexibility

Equation (12) cannot be used to compute $F_h(\bar{\omega})$ directly because Λ_h and ϕ_h are unknown. In our work, the approximate value of $F_h(\bar{\omega})$ is considered by using the power series expansion method.[8] An eigenvalue shifting technique is introduced to avoid the singularity of the stiffness matrix of a free–free structure and to accelerate the convergence rate of the power series. The dynamic flexibility matrix of a free–free structure is given by

$$F(\bar{\omega}) = (K - \bar{\omega}M)^{-1} = (K^* - \bar{\omega}^* M)^{-1} \tag{24a}$$

$$F(\bar{\omega}) = \phi(\Lambda^* - \bar{\omega}^* I)^{-1}\phi^T = \phi_k\left(\Lambda_k^* - \bar{\omega}^* I_k\right)^{-1}\phi_k^T + F_h(\bar{\omega}) \tag{24b}$$

where

$$F_h(\bar{\omega}) = \phi_h\left(\Lambda_h^* - \bar{\omega}^* I_h\right)^{-1}\phi_h^T = \phi_h(\Lambda_h - \bar{\omega} I_h)^{-1}\phi_h^T \tag{25}$$

$$K^* = K - \Delta\lambda M, \qquad \Lambda^* = \Lambda - \Delta\lambda I, \qquad \Lambda_k^* = \lambda_k - \Delta\lambda I_k$$

$$\Lambda_h^* = \Lambda_h - \Delta\lambda I_h, \qquad \bar{\omega}^* = \bar{\omega} - \Delta\lambda \tag{26}$$

where $\Delta\lambda$ is the eigenvalue shifting value. Now ϕ_k is divided into two subgroups, ϕ_1 and ϕ_2, and their corresponding eigenvalues are Λ_1^* and Λ_2^*, respectively. Here the diagonal elements in Λ_1^* and Λ_2^* are separately less and greater than $\bar{\omega}^*$. Expanding $F_h(\bar{\omega})$ as $A_0 + \bar{\omega}^* A_1 + \bar{\omega}^{*2} A_2 + \cdots$ and inserting it in Eq. (24b) yields

$$\begin{aligned} F(\bar{\omega}) &= \phi_k\left(\Lambda_k^* - \bar{\omega}^* I_k\right)^{-1}\phi_k^T + A_0 + \bar{\omega}^* A_1 + \bar{\omega}^{*2} A_2 + \cdots \\ &= \phi_1\left(\Lambda_1^* - \bar{\omega}^* I_1\right)^{-1}\phi_1^T + \phi_2\left(\Lambda_2^* - \bar{\omega}^* I_2\right)^{-1}\phi_2^T \\ &\quad + A_0 + \bar{\omega}^* A_1 + \bar{\omega}^{*2} A_2 + \cdots \\ &= -\bar{\omega}^{*-1}\phi_1\phi_1^T - \bar{\omega}^{*-2}\phi_1\Lambda_1^*\phi_1^T - \bar{\omega}^{*-3}\phi_1\Lambda_1^{*2}\phi_1^T - \cdots \\ &\quad + \phi_2\Lambda_2^{*-1}\phi_2^T + \bar{\omega}^*\phi_2\Lambda_2^{*-2}\phi_2^T + \bar{\omega}^{*2}\phi_2\Lambda_2^{*-3}\phi_2^T + \cdots \\ &\quad + A_0 + \bar{\omega}^* A_1 + \bar{\omega}^{*2} A_2 + \cdots \end{aligned} \tag{27}$$

in which

$$\Lambda_1^* = \Lambda_1 - \Delta\lambda I_1, \qquad \Lambda_2^* = \Lambda_2 - \Delta\lambda I_2 \tag{28}$$

From the definition of Eq. (24a), we have

$$(K^* - \bar{\omega}^* M)F(\bar{\omega}) = I \tag{29}$$

Embedding Eq. (27) into Eq. (29), collecting the terms with the same power of $\bar{\omega}^*$ on both sides of Eq. (29), and setting them equal to one another,[8] we can get

$$K^* A_0 = I - M\phi_k\phi_k^T \tag{30}$$

$$K^* A_p = M A_{p-1}, \qquad p \geq 1 \tag{31}$$

Although the stiffness matrix of a free structure is singular, the matrix K^* is nonsingular: It is a symmetric, sparse, and banded matrix. These properties are very useful for improving computational efficiency. In addition, Eq. (25) can be written as

$$\begin{aligned} F_h(\bar{\omega}) &= \phi_h(\Lambda_h - \bar{\omega} I_h)^{-1}\phi_h^T = \sum_{s=k+1}^{n} \frac{\phi_{hs}\phi_{hs}^T}{\lambda_{hs} - \bar{\omega}} \\ &= \sum_{s=k+1}^{n} \frac{\phi_{hs}\phi_{hs}^T}{\lambda_{hs}}\left[1 + \frac{\bar{\omega}}{\lambda_{hs}} + \left(\frac{\bar{\omega}}{\lambda_{hs}}\right)^2 + \cdots\right] \end{aligned} \tag{32}$$

Furthermore, Eq. (25) can also be written as

$$\begin{aligned} F_h(\bar{\omega}) &= \phi_h\left(\Lambda_h^* - \bar{\omega}^* I_h\right)^{-1}\phi_h^T = \sum_{s=k+1}^{n} \frac{\phi_{hs}\phi_{hs}^T}{\lambda_{hs}^* - \bar{\omega}^*} \\ &= \sum_{s=k+1}^{n} \frac{\phi_{hs}\phi_{hs}^T}{\lambda_{hs}^*}\left[1 + \frac{\bar{\omega}^*}{\lambda_{hs}^*} + \left(\frac{\bar{\omega}^*}{\lambda_{hs}^*}\right)^2 + \cdots\right] \end{aligned} \tag{33}$$

where $\lambda_{hs}^* = \lambda_{hs} - \Delta\lambda$. Actually, the convergence rate of Eq. (32) is nearly equivalent to that of the following geometric series:

$$\frac{1}{\lambda_{h,k+1} - \bar{\omega}} = \frac{1}{\lambda_{h,k+1}}\left[1 + \frac{\bar{\omega}}{\lambda_{h,k+1}} + \left(\frac{\bar{\omega}}{\lambda_{h,k+1}}\right)^2 + \cdots\right] \tag{34}$$

where $\lambda_{h,k+1}$ is the lowest frequency in λ_h. The convergence rate of Eq. (33) is nearly equal to that of the following geometric series:

$$\frac{1}{\lambda_{h,k+1}^* - \bar{\omega}^*} = \frac{1}{\lambda_{h,k+1}^*}\left[1 + \frac{\bar{\omega}^*}{\lambda_{h,k+1}^*} + \left(\frac{\bar{\omega}^*}{\lambda_{h,k+1}^*}\right)^2 + \cdots\right] \tag{35}$$

If the eigenvalue shifting value $\Delta\lambda$ is appropriately chosen so that $\bar{\omega}^*$ is small, the power series of Eq. (35) will converge more quickly in comparison with that of Eq. (34).

In short, the eigenvalue shifting technique has two advantages. First, the coefficient matrix before A_p ($p \geq 0$) on the left-hand side of Eqs. (30) and (31) will be the singular stiffness matrix K of a free–free structure without shifting. To avoid the singularity of the stiffness matrix K, in Refs. 9 and 10 K is changed to $(K + \eta M\phi_r\phi_r^T M)$, where ϕ_r are rigid-body modes and η is a properly chosen constant. In this case, that coefficient matrix suffers a lose of sparsity and bandedness. However, the eigenvalue shifting technique can save those advantages. Second, this technique can also improve the convergence rate.

Once A_p ($p \geq 0$) is obtained from Eqs. (30) and (31), the residual dynamic flexibility $F_h(\bar{\omega})$ can be given by

$$F_h(\bar{\omega}) = A_0 + \bar{\omega}^* A_1 + \bar{\omega}^{*2} A_2 + \cdots \tag{36}$$

Although $A_0, A_1, A_2, \ldots$ have no relation to ω, that is, A_p ($p \geq 0$) only need to be computed once for all different ω, they are closely related to $\Delta\lambda$ and are required to be recomputed when $\Delta\lambda$ is changed. Furthermore, the coefficient matrix K^* of Eqs. (30) and (31) should be redecomposed because K^* is also related to $\Delta\lambda$. To avoid choosing too many $\Delta\lambda$, group shifting is proposed, that is, the frequency range ($0 \leq \omega \leq \omega_k$) of the constrained structure is divided into subsections, and one shifting value $\Delta\lambda$ is chosen for each subsection. However, if a different shifting value $\Delta\lambda$ is chosen for a different $\bar{\omega}$, that is, individual shifting, the accuracy of constrained modes and frequencies will be much higher than with group shifting; however, individual shifting is more time consuming than the group shifting.

IV. Applications

As described in the introduction section, the effects of higher-order modes on the dynamic flexibility can also be obtained by the method developed in Ref. 9, that is,

$$F_h(\bar{\omega}) = \sum_{j=0}^{p} \bar{\omega}^{*j}(R_h M)^j R_h \tag{37}$$

in which R_h is obtained by solving the following equation:

$$K^* R_h = I - M\phi_k\phi_k^T \tag{38}$$

where p is the number of terms chosen according to the required accuracy. Comparison between Eqs. (30) and (38) shows that $R_h = A_0$.

Equation (21) is generally a nonlinear characteristic equation and can be solved by using the scheme described in Refs. 11 and 12. For a nonlinear characteristic equation, the number of sign changes of its Sturm sequence may not equal that of contained eignvalues. Furthermore, the number of contained eigenvalues cannot be determined from the modified Sturm sequence developed in Ref. 13 when the dynamic flexibility method is used to extract constrained modes. Therefore, the contained eigenvalues must be located by general searching together with Sturm's theorem. First, the frequency range from zero to the required maximum constrained frequency is divided into subsections, then general searching is conducted in each of the subsections. It is possible that one or more eigevalues are missed in a subsection. Then the subsection can be subdivided and researched. In most cases, this approach can locate quickly the contained eigenvalues because the analytical frequencies of constrained

structures can be used as a reference frame. In general, the method is only used to locate contained eigenvalues approximately, and the located eigenvalues should be further improved. Therefore, the shifting Rayleigh inverse iteration method[13] is employed to obtain constrained mode shapes and to improve frequencies. To prevent the iterative process from converging to undesired modes, Gram–Schmidt orthogonalization is employed. The fixed-point weighting technique[11] is also introduced to make the iterative process converge to desired eigenvalues with a probability as large as possible when the initial iterative values are far away from actual eigenvalues.[12] Denoting the initial iterative values of the sth eigenpairs as $\{\bar{\omega}_s^{(0)}, Q_s^{(0)}\}$, we define the fixed-point weighting procedure as follows:

$$\left\lfloor \bar{K}\left(\bar{\omega}_s^{(0)}\right) - \bar{\omega}_s^{(0)}\bar{M}\left(\bar{\omega}_s^{(0)}\right)\right\rfloor \left\{z_s^{(i)}\right\} = \left\{z_s^{(i-1)}\right\}, \qquad i = 1, 2, \ldots, \alpha \tag{39}$$

Finally, we assume $\{Q_s^{(0)}\} = \{z_s^{(\alpha)}\}$. Then, $\bar{\omega}_s^{(0)}$ and $\{Q_s^{(0)}\}$ are used as the initial iterative values for shifting Rayleigh inverse iteration. This iterative process and its convergence may be found in Ref. 13.

If a linear characteristic equation is desired, only the term that has no relation to the frequency ω on the right-hand side of Eq. (36), that is, A_0 is retained. Then one has

$$F_h(\bar{\omega}) \approx A_0 \tag{40}$$

This approximation is equivalent to the result of Eq. (32) when $\bar{\omega} \ll \lambda_{h,k+1}$,

$$F_h(\bar{\omega}) \approx \phi_h \Lambda_h^{-1} \phi_h^T \tag{41}$$

This approximation results in poor accuracy of the derived constrained modes; however, it is very convenient for computation. If better accuracy is required, higher power terms of $\bar{\omega}^*$ on the right-hand side of Eq. (36), for example, up to $\bar{\omega}^{*2}$ or $\bar{\omega}^{*3}$, have to be taken in the computations. Then Eq. (21) remains a nonlinear characteristic equation. It is fortunate that the dimension of the eigenequation, as shown in Eq. (21), is small, and solving the equation is not time consuming.

As shown in Eqs. (17) and (36), only the matrices $\bar{A}_p$, $p = 1, 2, \ldots$, formed by the columns of $\bar{A}_p$, $p = 1, 2, \ldots$, that are associated with the boundary degree of freedom are required in Eqs. (30) and (31) for determining the coefficient matrices of the power series expansion of $F_h(\bar{\omega})$. Then we have

$$F_{h,b} = \bar{A}_0 + \bar{\omega}^* \bar{A}_0 + \bar{\omega}^{*2} \bar{A}_0 + \cdots \tag{42}$$

Thus, the computational time can be cut down dramatically because the number of boundary degree of freedom is often small.

There may be a big difference between the free test modes ϕ_k and the analytical ones of a free structure. This suggests that the error of the stiffness matrix K should be large when the accuracy of the mass matrix is assumed to be good. Then the matrix K has to be updated so that the modes of the updated K and M conform with ϕ_k. This will ensure the accuracy of the derived constrained modes. Would it be possible simply to update the model and use it to predict the constrained modes and frequencies? This is not a good method for that purpose because the model updating techniques at present cannot realize the connectivity of the finite element model perfectly. Though the modes of the updated K and M of free structures conform with ϕ_k, the satisfied constrained modes and frequencies would not be derived definitely from the submatrix K_{ii} and M_{ii} of K and M.

V. Numerical Example

The structure, as shown in Fig. 2, is a seven-bay space truss. Each bay of the truss is a cube with the side dimension of 0.3 m. The truss contains 96 bar members, which are made of aluminum tubes with a diameter of $\Phi 6 \times 1$ mm. Young's modulus of elasticity and the mass density of the bar members are 72.7 GN/m^2 and 3100 kg/m^3, respectively. Each of nodes is added with a centralized mass of 0.6 kg. The number of degrees of freedom is 96 when it is a free structure. The constrained modes are derived by the dynamic flexibility method when the truss is clamped at nodes 1, 2, 3, and 4, in which the number of boundary degrees of freedom is 12. The analytical eigenpairs of the constrained structure are assumed as the exact values of the constrained modes and frequencies, that is, ω_{ct}

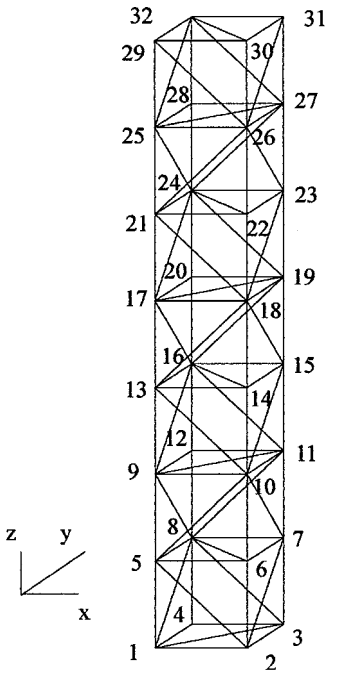

Fig. 2 Space truss structure.

and x_{ct}, whereas the analytical lower-order modes and frequencies of the free structure are taken as test cases. The cases of solving the linear and nonlinear characteristic equation are discussed. The error indices are defined as

$$\omega_c\% = \frac{\omega_c - \omega_{ct}}{\omega_{ct}}\%, \qquad \|x_c\|\% = \sqrt{\frac{\|x_c x_{ct}\|}{\|x_{ct}\|}}\%$$

$$\text{MAC} = \frac{\left|x_{ct}^T x_c\right|}{\|x_{ct}\| \times \|x_c\|} \tag{43}$$

where MAC is Modal Assurance Criteria.

A. Solving a Linear Characteristic Equation

In this case, $F_h(\bar{\omega}) \approx A_0$. Figure 3 shows that the errors of the derived constrained modes vary with different shifting values $\Delta\lambda$ when all six rigid-body modes and the first three lower-order free–free flexible modes are used in analysis. The symbols in Fig. 3 indicate the error curve of the first to ninth modes. It can be seen from Fig. 3 that the accuracy of the derived constrained modes varies closely with $\Delta\lambda$. When $\Delta\lambda$ is close to a certain constrained frequency, the error of the corresponding derived modes and frequencies is low. From this observation, the errors of each constrained mode and frequency will be lower if $\Delta\lambda$ is properly chosen and the individual shifting technique is used. For group shifting, it is recommended that $\Delta\lambda$ be close to the lowest frequency of the group so that the errors of the lower-order modes are small.

B. Solving a Nonlinear Characteristic Equation

Two shifting techniques are discussed for the case $F_h(\bar{\omega}) = A_0 + \bar{\omega}^* A_1 + \bar{\omega}^{*2} A_2 + \cdots$.

1. Group Shifting

The shifting value is chosen as 0.4×10^5 (rad/s)^2 when computing the first to third modes. For all other modes, 1.0×10^5 (rad/s)^2 is chosen. The constrained modes that are obtained using six rigid-body modes and three or five free test flexible modes are listed in Table 1 when the power series is truncated at the term with $\bar{\omega}^{*2}$ or $\bar{\omega}^{*3}$. The 8th and 13th columns of Table 1 show the number of iterations for solving the nonlinear characteristic equation. Some conclusions can be drawn from Table 1.

1) It is shown that $\|x_c\|\%$ is a more sensitive index than MAC.

2) Generally, the errors of the constrained frequencies are lower than those of the constrained mode shapes. The errors of the constrained modes determine whether the constrained frequencies and mode shapes can be used in the following analysis such as model improvement, loads analysis, etc.

3) The number of iterations for solving the nonlinear characteristic equation is often 2–4. When the shifting value $\Delta\lambda$ is appropriate,

Table 1 Results obtained by the group sifting technique, six rigid-body modes and three (five) free test flexible modes

Mode no.	Free frequency, Hz	Constrained frequency, Hz	$F_h(\bar{\omega}) = A_0 + \bar{\omega}^* A_1 + \bar{\omega}^{*2} A_2$					$F_h(\bar{\omega}) = A_0 + \bar{\omega}^* A_1 + \bar{\omega}^{*2} A_2 + \bar{\omega}^{*3} A_3$				
			ω_c, Hz	ω_c, %	$\|x_c\|$, %	MAC	Number of iterations	ω_c, Hz	ω_c, %	$\|x_c\|$, %	MAC	Number of iteration
1	0	11.4162	11.4162	0.0	0.20	1.00	3	11.4162	0.0	0.05	1.00	3
			(11.4162)	(0.0)	(0.20)	(1.00)	(3)	(11.4162)	(0.0)	(0.05)	(1.00)	(3)
2	0	11.5918	11.5918	0.0	0.23	1.00	2	11.5918	0.0	0.07	1.00	2
			(11.5918)	(0.0)	(0.05)	(1.00)	(2)	(11.5918)	(0.0)	(0.01)	(1.00)	(2)
3	0	31.3209	31.3209	0.0	0.0	1.00	2	31.3209	0.0	0.0	1.00	2
			(31.3209)	(0.0)	(0.0)	(1.00)	(2)	(31.3209)	(0.0)	(0.0)	(1.00)	(2)
4	0	51.8845	51.8845	0.0	0.02	1.00	2	51.8845	0.0	0.0	1.00	2
			(51.8845)	(0.0)	(0.01)	(1.00)	(2)	(51.8845)	(0.0)	(0.0)	(1.00)	(2)
5	0	54.7788	54.7788	0.0	0.12	1.00	3	54.7788	0.0	0.02	1.00	3
			(54.7788)	(0.0)	(0.12)	(1.00)	(3)	(54.7788)	(0.0)	(0.02)	(1.00)	(3)
6	0	79.7031	79.7038	0.0	4.60	1.00	3	79.7032	0.0	2.58	1.00	2
			(79.7031)	(0.0)	(3.54)	(1.00)	(3)	(79.7031)	(0.0)	(1.64)	(1.00)	(3)
7	56.8960	91.3943	91.5229	0.14	20.41	0.9991	4	91.4339	0.04	15.25	0.9997	4
			(91.3944)	(0.0)	(3.36)	(1.00)	(3)	(91.3943)	(0.0)	(1.77)	(1.00)	(3)
8	57.2083	109.3067	110.5710	1.16	37.34	0.9902	4	110.0201	0.65	32.45	0.9944	5
			(109.3090)	(0.0)	(6.09)	(1.00)	(3)	(109.3073)	(0.0)	(4.34)	(1.00)	(3)
9	58.2405	117.4818	119.2038	1.47	38.77	0.9886	9	118.4818	0.85	33.86	0.9934	8
			(117.4819)	(0.0)	(3.29)	(1.00)	(3)	(117.4818)	(0.0)	(2.09)	(1.00)	(3)
10	112.0155	143.8776	(144.0494)	(0.12)	(24.63)	(0.9982)	(4)	(143.9387)	(0.04)	(19.13)	(0.9993)	(4)
11	113.1383	156.8431	(157.5038)	(0.42)	(32.73)	(0.9942)	(12)	(157.2034)	(0.23)	(27.95)	(0.9969)	(13)

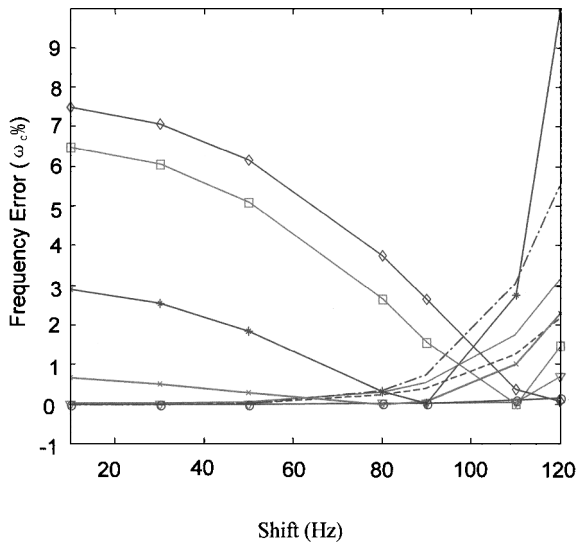

Errors of constrained frequencies varies with different shifting values $\Delta\lambda$

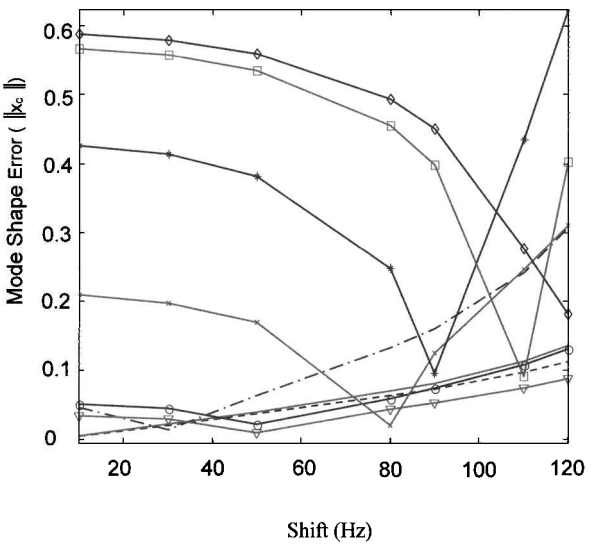

Errors of constrained modes varies with different shifting values $\Delta\lambda$

Fig. 3 Errors of constrained modes.

the number of iterations is smaller, whereas the number becomes larger when $\Delta\lambda$ is not properly chosen.

4) The errors of the constrained modes will be lower if the number of the terms retained in the power series or the number of used free test modes is larger.

5) If the accuracy requirements $\omega_c\% < 1\%$, $\|x_c\|\% < 5\%$, and MAC > 0.99 are satisfied, the frequency criterion introduced in Ref. 14 can be used to decide how many free test modes should be required. From Ref. 14, one can get

$$\omega_f \leq \beta\omega_{c,\max} \tag{44}$$

where ω_f is the largest free frequency taken in the computation and $\omega_{c,\max}$ is the largest constrained frequency that meets the accuracy requirements. A conservative value $\beta = 1.5$ is recommended in Ref. 14. The values of β obtained by the group shifting technique are listed in Table 2. It is clear that all β are less than 1.5. Although the values of β when five free test flexible modes are used are larger than those when three modes are taken in the analysis, more derived constrained modes are satisfied with the accuracy requirements in the former situation. It can be seen from Table 1 that the dynamic flexibility method will meet the accuracy requirements, but only a few free test modes are required because the effects of higher-order modes on the dynamic flexibility are considered.

2. Individual Shifting

In the group shifting technique, it is difficult to subdivide the constrained frequency range properly. In addition, the error of certain constrained frequency may be large when the shifting value is far away from that constrained frequency. To improve the accuracy of the derived constrained modes, the individual shifting technique can be used. The constrained modes obtained by the individual shifting technique are listed in Table 3. The conclusions are nearly the same as those of the group shifting technique. However, the accuracy of the constrained modes as shown in Table 3 is much better than that in Table 1. The first 9 constrained modes obtained with three free test flexible modes and the first 11 constrained modes obtained with five free test flexible modes satisfy the accuracy requirements already described. When six rigid-body modes and three free test flexible modes are used for the computation, we have $\omega_f = 58.2405$ Hz and $\omega_{c,\max} = 117.4818$ Hz, then $\beta = 0.50$. When six rigid-body modes and five free test flexible modes are taken in analysis, one gets $\omega_f = 113.1383$ Hz and $\omega_{c,\max} = 156.8431$ Hz, so that $\beta = 0.72$. It is clear that all β obtained by the individual shifting technique are smaller than those obtained by the group shifting technique with the same conditions. As a result, fewer free test modes are required to meet the same accuracy requirements in the individual shifting technique.

Table 2 Values of β obtained by group shifting technique

	$F_h(\bar{\omega}) = A_0 + \bar{\omega}^* A_1 + \bar{\omega}^{*2} A_2$			$F_h(\bar{\omega}) = A_0 + \bar{\omega}^* A_1 + \bar{\omega}^{*2} A_2 + \bar{\omega}^{*3} A_3$		
Six rigid-body modes	ω_f, Hz	$\omega_{c,\max}$, Hz	β	ω_f, Hz	$\omega_{c,\max}$, Hz	β
+Three free test modes	58.2405	79.7031	0.73	58.2405	79.7031	0.73
+Five free test modes	113.1383	91.3943	1.24	113.1383	117.4818	0.96

Table 3 Results obtained by the individual sifting technique, six rigid-body and three (five) free test flexible modes

			$F_h(\bar{\omega}) = A_0 + \bar{\omega}^* A_1 + \bar{\omega}^{*2} A_2$					$F_h(\bar{\omega}) = A_0 + \bar{\omega}^* A_1 + \bar{\omega}^{*2} A_2 + \bar{\omega}^{*3} A_3$				
Mode no.	Free frequency, Hz	Constrained frequency, Hz	ω_c, Hz	ω_c, %	$\|x_c\|$, %	MAC	Number of iterations	ω_c, Hz	ω_c, %	$\|x_c\|$, %	MAC	Number of iterations
1	0	11.4162	11.4162	0.0	0.0	1.00	3	11.4162	0.0	0.0	1.00	3
			(11.4162)	(0.0)	(0.0)	(1.00)	(3)	(11.4162)	(0.0)	(0.0)	(1.00)	(3)
2	0	11.5918	11.5918	0.0	0.0	1.00	2	11.5918	0.0	0.0	1.00	2
			(11.5918)	(0.0)	(0.0)	(1.00)	(2)	(11.5918)	(0.0)	(0.0)	(1.00)	(2)
3	0	31.3209	31.3209	0.0	0.0	1.00	2	31.3209	0.0	0.0	1.00	2
			(31.3209)	(0.0)	(0.0)	(1.00)	(2)	(31.3209)	(0.0)	(0.0)	(1.00)	(2)
4	0	51.8845	51.8845	0.0	0.02	1.00	2	51.8845	0.0	0.0	1.00	2
			(51.8845)	(0.0)	(0.01)	(1.00)	(2)	(51.8845)	(0.0)	(0.0)	(1.00)	(2)
5	0	54.7788	54.7788	0.0	0.06	1.00	3	54.7788	0.0	0.01	1.00	3
			(54.7788)	(0.0)	(0.06)	(1.00)	(3)	(54.7788)	(0.0)	(0.01)	(1.00)	(3)
6	0	79.7031	79.7031	0.0	0.01	1.00	2	79.7031	0.0	0.01	1.00	2
			(79.7031)	(0.0)	(0.01)	(1.00)	(2)	(79.7031)	(0.0)	(0.01)	(1.00)	(2)
7	56.8960	91.3943	91.3943	0.0	2.26	1.00	3	91.3943	0.0	0.85	1.00	3
			(91.3943)	(0.0)	(0.15)	(1.00)	(3)	(91.3943)	(0.0)	(0.03)	(1.00)	(3)
8	57.2083	109.3067	109.3067	0.0	4.03	1.00	3	109.3067	0.0	2.36	1.00	3
			(109.3067)	(0.0)	(0.06)	(1.00)	(3)	(109.3067)	(0.0)	(0.01)	(1.00)	(3)
9	58.2405	117.4818	117.4818	0.0	3.40	1.00	3	117.4818	0.0	2.16	1.00	3
			(117.4818)	(0.0)	(3.29)	(1.00)	(3)	(117.4818)	(0.0)	(2.09)	(1.00)	(3)
10	112.0155	143.8776	(143.8776)	(0.0)	(1.76)	(1.00)	(3)	(143.8776)	(0.0)	(0.56)	(1.00)	3
11	113.1383	156.8431	(156.8431)	(0.0)	(3.40)	(1.00)	(3)	(156.8431)	(0.0)	(1.77)	(1.00)	(3)

When the linear characteristic equation is solved with six rigid-body modes and three free test flexible modes, the computational time is 0.14 s using a Pentium-Pro180. Although the nonlinear characteristic equation is solved with the same number of modes and the power series truncated at the term with $\bar{\omega}^{*2}$, the computational time when using the group shifting or the individual shifting techniques is 3.86 and 5.33 s, respectively. It is true that the computational time is the highest for solving the nonlinear characteristic equation with the individual shifting technique; however, its accuracy is the best.

VI. Conclusions

A method for extracting constrained modes from free test data is successfully developed based on experimental and theoretical modeling. Two methods for taking into consideration the effects of neglected higher-order modes on the dynamic flexibility are discussed. The applicability of the methods is examined. The following conclusions can be drawn from the dynamic flexibility method.

1) The effects of higher-order modes on the dynamic flexibility are expanded as a power series to avoid repeatedly computing the inverse shown in Eq. (24a). The number of power terms can be chosen according to the accuracy requirements. It is advised that the power series be taken up, at most, to the term with $\bar{\omega}^{*3}$.

2) The number of free test modes required in analysis is very small because of the consideration of the effects of neglected higher-order modes on the dynamic flexibility. This shows that the number of extracted usable constrained modes is greater than that of free test flexible modes used.

3) The eigenvalue shifting technique not only avoids the singularity of the stiffness matrix of a free–free structure but improves the computational efficiency as well.

4) The accuracy of the constrained modes obtained by the individual shifting technique is higher than that obtained by the group shifting scheme, but the former needs more computational time.

Acknowledgments

The support of the National Natural Science Foundation of China, under Grant 59675015, is highly appreciated. This research work was performed at the Institute of Vibration Engineering, Nanjing University of Aeronautics and Astronautics.

References

[1]Przemieniecki, J. S., *Theory of a Matrix Structural Analysis,* McGraw–Hill, New York, 1968, pp. 357–359.

[2]Zhang, O., and Zerva, A., "Extraction of Free–Free Modes Using Constrained Test Data," *AIAA Journal*, Vol. 33, No. 2, 1995, pp. 2440–2442.

[3]Zhang, D. W., "A Galerkin Method for Transforming Constrained-Structure Test Modes to Free Structure Test Modes," *Acta Astronautica Sinica*, Vol. 7, No. 4, 1988, pp. 64–69.

[4]Zhang, D. W., "Extraction of Free–Free Modes Using Constrained-Structure Test Modes—Free Force of the Boundary Degrees of Freedom," *Proceedings of the 5th Modal Analysis and Experiment Conference,* Shanghai Jiaotong Univ., Shanghai, PRC, 1988, pp. 762–769.

[5]Blair, M. A., and Vadlamudi, N., "Constrained Structural Dynamic Model Verification Using Free Vehicle Suspension Testing Methods," *Proceedings of the AIAA/ASME/ASCE/AHS/ASC Structures, Structural Dynamics, and Materials Conference*, AIAA, Washington, DC, 1988, pp. 1187–1193.

[6]Admire, J. R., Tinker, M. L., and Ivey, E. W., "Mass-Additive Modal Test Method for Verification of Constrained Structural Models," *AIAA Journal*, Vol. 31, No. 11, 1993, pp. 2148–2153.

[7]Admire, J. R., et al., "Residual Flexibility Test Method for Verification of Constrained Structural Models," *AIAA Journal*, Vol. 32, No. 1, 1994, pp. 170–175.

[8]Zhang, D. W., and We, F. S., "Efficient Computation of Many Eigenvector Derivatives Using Dynamic Flexibility Method," *AIAA Journal*, Vol. 35, No. 4, 1997, pp. 712–718.

[9]Zhang, D. W., and Wei, F. S., "Computation of Eigenvector Derivatives Using Higher-Precision Dynamic Flexibility Expression," *Journal of Aerospace Engineering*, Vol. 3, No. 2, pp. 69–75.

[10]Hu, H. C., *Vibration Theory of Multi-Degree of Freedom System*, Science Press, Beijing, 1987, pp. 108–110.

[11]Xu, Q. Y., and Luo, X. Y., "An Improved Algorithm for Solving Non-Linear Eigenvalue Problem of Dynamic Substructure," *Computational Structural Mechanics and Applications*, Vol. 4, No. 1, 1987, pp. 23–32.

[12]Zhang, D. W., "A New Analysis Method for Dynamic Substructure Coupling—Accurate Free Interface Method," *Proceedings of the 5th Vibration Theory and Applications Conference*, Nanjing Univ. of Aeronautics and Astronautics, Nanjing, PRC, 1993, pp. 19–26.

[13]Wittrick, W. H., and Williams, F. W., "A General Algorithm for Computing Natural Frequencies of Elastic Structures," *Quarterly Journal of Mechanics and Applied Mathematics*, Vol. 24, Pt. 3, 1971, pp. 263–284.

[14]Liu, G. G., Li, J. J., and Zhang, D. W., "Multi-Level Substructural Analysis in Modal Synthesis—Two Improved Substructural Assembling Techniques," *Acta Aeronautica Sinica*, Vol. 3, No. 4, 1982, pp. 28–35.

A. Berman
Associate Editor